DETERMINATION OF MEAN SURFACE POSITION AND SEA STATE FROM THE RADAR RETURN OF A SHORT-PULSE SATELLITE ALTIMETER

16

Donald E. Barrick
BATTELLE
Columbus Laboratories
505 King Avenue
Columbus, Ohio 43201

Using the specular point theory of scatter from a very rough surface, the average backscatter cross section per unit area per radar cell width is derived for a cell located at a given height above the mean sea surface. This result is then applied to predict the average radar cross section observed by a short-pulse altimeter as a function of time for two modes of operation: pulse-limited and beam-limited configurations. For a pulse-limited satellite altimeter, a family of curves is calculated showing the distortion of the leading edge of the receiver output signal as a function of sea state (i.e., wind speed). A signal processing scheme is discussed that permits an accurate determination of the mean surface position--even in high seas--and, as a by-product, the estimation of the significant seawave height (or wind speed above the surface). Comparison of these analytical results with experimental data for both pulse-limited and beam-limited operation lends credence to the model. Such a model should aid in the design of short-pulse altimeters for accurate determination of the geoid over the oceans, as well as for the use of such altimeters for orbital sea-state monitoring.

INTRODUCTION

Sea surface roughness has always represented an unavoidable degradation to the performance of a satellite radar altimeter[1,2]*. It would be desirable for geodetic purposes to measure the position of the mean sea surface to an accuracy of less than a foot. Sea states over the oceans result in waveheights commonly of the order of six or more feet. It is physically obvious that such waveheights will "stretch" the receiver output pulse in some way, producing an uncertainty in the position of the mean surface of the order of the sea waveheight. Since sea state at any given time and place on the ocean is usually unknown, and since the interaction mechanism of an altimeter pulse with the sea has not yet been fully analyzed, doubt has remained as to the efficacy of an altimeter to determine mean sea level to the precision geodetically desired.

It is the purpose of this paper to show that sea state effects on altimeter performance need not limit its accuracy, primarily because the interaction between the radar pulse and the ocean waves is understood and predictable. Using a physically simple but rigorous theory, we intend to analyze the pulse distortion from wind-driven sea waves. The validity of the results will be established by comparison with two independent sets of experimental data.

Based upon the acceptance of the analysis set forth herein, we feel that mean sea level can be extracted from a satellite altimeter receiver signal. A simple one-step process will be suggested, whereby the incoherent, averaged signal versus time is differentiated, and the mean level is seen immediately as the position of the peak. The rms ocean waveheight and/or wind speed responsible for the ocean waves can then be inferred directly from the width of this signal derivative pulse.

PHYSICAL THEORY RESPONSIBLE FOR SCATTER

For the microwave frequencies at which an altimeter will operate, scatter from the sea within the near-vertical region directly beneath the satellite is quasi-specular in nature. This means that such scatter is produced primarily by specular or glitter points on the surface whose normals point toward the satellite. This is the same mechanism producing the dancing glitter of sunlight or moonlight on a water surface. Such scatter persists only as far as 15-20° from the vertical, since gravity waves can seldom maintain slopes greater than this amount before they break and dissipate energy. A physical picture of the specular points illuminated within a short-pulse radar cell advancing at an angle θ with respect to the mean surface is shown in Figure 1.

This specular point scatter is readily predictable from geometrical and/or physical optics principles, and has been analyzed by this author previously[3]. Here we extend the theory to include the height of the surface, since the short radar pulse will not illuminate the entire surface at a given time, but only those waves whose heights are sufficient to lie within the radar pulse. As the starting point, we note both from elementary geometrical optics principles or from more rigorous

*References are given on page 19.

physical optics derivations[3,4], that the field scattered from N specular points (expressed in terms of the square root of the backscatter cross section) is

$$\sigma_B^{1/2} = \sum_{i=1}^{N} \pi^{1/2} g_i^{1/2} e^{i2k_o h_i \cos\theta} \quad , \tag{1}$$

where g_i is the Gaussian curvature at the i-th specular point, i.e., $g_i = |\rho_{1i}\rho_{2i}|$, with ρ_{1i} and ρ_{2i} as the principal radii of curvature at this point. Also, h_i is the height of the i-th specular point above the mean surface (taken as k = 0), θ is the angle of incidence from the vertical, and $k_o = 2\pi/\lambda$ is the free-space radar wavenumber, λ being the wavelength.

Now, we square the above equation and average with respect to the phase, φ_{ij}, noting that $\varphi_{ij} = 2k_o \cos\theta(h_i + h_j)$ will be uniformly distributed between zero and 2π as long as the sea waveheight is larger than the radar wavelength. Thus the average of the double summation over i and j is zero except where j = -i, reducing the result to a single summation:

$$\langle\sigma_B\rangle_{ph} = \pi \sum_{i=1}^{N} g_i \quad . \tag{2}$$

Now, we rewrite this equation in integral form as a distribution of specular points versus height above the surface, h, and Gaussian curvature, g, as

$$\langle\sigma_B\rangle_{ph} = \pi A \int_{-\infty}^{\infty} dh \int_{0}^{\infty} N(h,g) g \, dg \quad , \tag{3}$$

where AN(h,g) is the number of specular points within a surface patch of area A, within the height interval h to h + dh, and with Gaussian curvatures between g and g + dg.

We now complete the averaging process by defining $n(h,g) \equiv \langle N(h,g)\rangle$ as the average specular point density, and we then denote $\eta_o(h)$ as the average radar cross

section per unit area of the surface per unit height increment, Δh, at a given height h; thus we have

$$\eta^o(h) = \pi \int_0^\infty n(h,g)\ g\ dg \quad . \tag{4}$$

Here we employ the normalization $\sigma^o = \int_{-\infty}^{\infty} \eta^o(h)dh$, where σ^o is the standard average backscatter cross section per unit area. Thus, a short pulse producing a vertical radar resolution cell of width Δh at height h will produce, on the average, a radar cross section per unit area of $\eta^o(h)\Delta h$.

The specular point density, n, can readily be determined (almost by inspection) from the work of Barrick[3] preceding Eq. (7) of that paper; one must merely include height in the probability densities. Thus the density of specular points within area A is

$$n(h,g)\ dg = p(h,\zeta_{xsp},\zeta_{ysp},\zeta_{xx},\zeta_{yy},\zeta_{xy})\,|\zeta_{xx}\zeta_{yy} - \zeta_{xy}^2|\,d\zeta_{xx}d\zeta_{yy}d\zeta_{xy} \quad , \tag{10}$$

where p is the joint probability density function of the surface height h, the surface slopes ζ_x, ζ_y, and the second partial derivatives of the surface at a given surface point. Since it is known a priori that scatter is originating at surface regions with their normals pointing toward the satellite, the slopes which must be used are geometrically known; we denote them ζ_{xsp} and ζ_{ysp}.

Likewise, the Gaussian curvature at a specular point is found from differential geometry to be

$$g = \frac{(1 + \zeta_{xsp}^2 + \zeta_{ysp}^2)^2}{|\zeta_{xx}\zeta_{yy} - \zeta_{xy}^2|} \quad . \tag{11}$$

Hence we arrive at the result

$$\eta^o(h) = \pi \iiint_{-\infty}^{\infty} |\zeta_{xx}\zeta_{yy} - \zeta_{xy}^2|\,p(h,\zeta_{xsp},\zeta_{ysp},\zeta_{xx},\zeta_{xy},\zeta_{yy}) \times$$

$$\frac{(1 + \zeta_{xsp}^2 + \zeta_{ysp}^2)^2}{|\zeta_{xx}\zeta_{yy} - \zeta_{xy}^2|}\, d\zeta_{xx}d\zeta_{yy}d\zeta_{xy}$$

$$= \pi(1 + \zeta_{xsp}^2 + \zeta_{ysp}^2)^2\ p(h,\zeta_{xsp},\zeta_{ysp}) \tag{12}$$

For backscatter, the squared factor in parentheses is merely equal to $\sec^4 \theta$, where θ is the incidence angle from the vertical. Also, it is simple to show that, while the surface height h and second derivatives are correlated, the height and slopes are uncorrelated. Hence, if the surface is Gaussian (or nearly so, which is true for the sea), the height and slopes are statistically independent and we have

$$\mathcal{P}(h) = \pi \sec^4 \theta \; p(h) p(\zeta_{xsp}, \zeta_{ysp}) \quad , \tag{13}$$

where p(h) is the height probability density and $p(\zeta_x, \zeta_y)$ is the joint slope probability density. The above result can now be applied to predict the average radar cross section observed at a short-pulse altimeter as a function of time.

APPLICATION TO SHORT-PULSE SATELLITE ALTIMETER

1. General Development

We now apply Eq. (13) to the problem depicted in Fig. 2: a satellite at altitude H emitting a spherical pulse which in turn sweeps past a spherical earth. The spatial pulse width for a backscatter radar is $c\tau/2$, where c is the velocity of light and τ is the time width of the pulse (compressed, if applicable) at the receiver output. Likewise, the distance of the spherically emanating pulse from the satellite, measured in time at the receiver from transmission of the signal, is ct/2. However, for convenience, we henceforth choose t = 0 as the time that the center of the spherical pulse shell strikes the uppermost cap of the spherical earth. In other words, in the absence of any roughness, the received pulse from the suborbital point will be a replica of the processed transmitter pulse, and we choose its center time position as a reference in order to study the effect of sea state on pulse distortion.

First of all, we note from Fig. 2 that the angle of incidence, θ, at any point on the surface is given by $\theta \approx \psi + \varphi \simeq \psi(1 + H/a)$ for θ small. The incidence angle at the intersection of the mean earth spherical surface and the center of the pulse cell, expressed in terms of receiver time is then $\theta \simeq \sqrt{(ct/H)(1 + H/a)}$. For a short pulse, θ can be considered a constant within the pulse cell width. The height, h, to a point at the center of the cell above the mean sea surface can then be given as

$$h = \frac{H(1 - \cos \psi) + a(1 - \cos \varphi) - (ct/2)\cos \psi}{\cos \varphi} \tag{14}$$

and for ψ small, this reduces to

$$h \simeq \frac{H}{2} \psi^2 \left(1 + \frac{H}{a}\right) - \frac{ct}{2} \quad . \tag{15}$$

At this point, we must make some assumptions about the surface statistics and radar properties in order to perform the integration. For the sake of studying the general nature of the radar return, we make the following assumptions: (i) the signal shape is flat, of width τ, and zero everywhere else, (ii) the antenna beam pattern is uniform out to ψ_B off the axis, and zero everywhere else; ψ_B is thus the half-power half-beamwidth of the antenna*. We assume also that the sea surface height and slope probability distributions are Gaussian, realizing of course that the height distribution to second order is not quite Gaussian, but slightly skewed from the symmetric Gaussian shape, and has less probability in the tails. Furthermore, we assume that the sea is nearly isotropic, making the slopes ζ_x and ζ_y independent of wind direction. This is quite valid for very small incidence angles (and hence specular slopes).

Thus we have

$$p(\zeta_{xsp},\zeta_{ysp}) = p(\tan\theta) = \frac{1}{\pi s^2} e^{-\frac{\tan^2\theta}{s^2}} , \qquad (16)$$

and

$$p(h) = \frac{1}{\sqrt{2\pi}\,\sigma_h} e^{-\frac{h^2}{2\sigma_h^2}} , \qquad (17)$$

where $s^2 = \langle\zeta_x^2\rangle + \langle\zeta_y^2\rangle$ and $\sigma_h^2 = \langle h^2\rangle$.

Later, when relating these quantities to wind-developed waves, we shall use the relationships

$$s^2 = 5.5 \times 10^{-3}\, v \quad \text{and} \quad \sigma_h^2 = 2.55 \times 10^{-4}\, v^4 , \qquad (18)$$

where v is wind velocity in meters per second. The first of these relationships is inferred empirically from slope data versus wind speed presented in Phillips[5], and the second is obtained from integrating the Phillips wind-wave height spectrum.

Thus, the observed average radar cross section as a function of time will be

$$\sigma(t) = 2\pi^2 a^2 \int_0^{\frac{H}{a}\psi_B} p(\tan\theta)\sec^4\theta \sin\varphi \left\{ \int_{h-\frac{\Delta h}{2}}^{h+\frac{\Delta h}{2}} p(h)dh \right\} d\varphi , \qquad (19)$$

where θ and h were related to φ previously.

*Other, possibly more realistic, pulse and beam shapes can be readily inserted into the integral if desired.

For a pulse width sufficiently short that $\Delta h \approx (c\tau/2) < 2\sigma_h$, we can approximate the second integral and obtain a closed-form answer for the remaining integral. Physically, this requires that the spatial pulse width be less than the rms ocean waveheight (peak-to-trough). This is realized on the open ocean with compressed pulse widths less than about 10 ns for waves excited by winds greater than about 10 knots. For simplicity we shall make this assumption here, analyzing the more general case at a later date. The result is then

$$\sigma(t) = \frac{\pi c \tau}{2s^2[(1/a) + (1/H)]} \left\{ \operatorname{erf}\left(\frac{ct}{\sqrt{8}\,\sigma_h}\right) + \operatorname{erf}\left(\frac{H'\psi_B^2 - ct}{\sqrt{8}\,\sigma_h}\right) \right\} , \qquad (20)$$

where $H' = H[1 + (H/a)]$. The quantities in the braces are the error functions; the first one is responsible for the rising leading edge of the radar return, while the second produces the fall-off of the trailing edge.

2. Pulse-Limited Altimeter ($\psi_B \gg \sqrt{c\tau/H'}$)

When the radar is sufficiently high, the beamwidth sufficiently wide, and the pulse length sufficiently short, the response of the altimeter is said to be pulse-limited. This means in effect that the earth area illuminated most of the time lies in a "range ring" of constant surface area, as shown in Fig. (3a). Such a situation will always exist for a short-pulse satellite altimeter, will nearly always exist for aircraft altimeters, but may not exist for tower-based altimeters looking at the sea (an example of the latter will be discussed subsequently). The general form of Eq. (20) is valid for either pulse- or beam-limited operation, under the simplifying assumptions made previously (flat pulse and antenna pattern, short-pulse operation).

In this mode of operation, the mean surface at the suborbital point lies somewhere in the leading, rising edge of the echo. The essence of the problem, however, is that the rise time of the leading edge is not only inversely proportional to the transmitted signal bandwidth (or shape)--a factor which could easily be removed for high signal-to-noise ratios because the signal shape is known a priori--but the rise time varies also with sea state because of temporal dispersion caused by the spatial distribution of specular points.

To study the theoretical shape of the leading edge of the return for the pulse-limited case, we examine Eq. (20). First of all, we note that the return rises rapidly to a maximum, has a flat shape in the middle of duration $t_D = (H'/c)\ \psi_B^2$, and falls off to zero as rapidly as it rose. The shape of the pulse is symmetric about $t_D/2$. In practice, such a flat, symmetric return will not be observed, primarily because the antenna pattern falls off with increasing ψ, rather than remaining constant out to ψ_B and then dropping suddenly to zero, as we assumed here. The shape shown in Fig. 3a is more typical of the overall echo shape. The shape of this latter portion of the signal need not concern us here, however, because it contains no information about the mean surface position and little information about sea state. The maximum value of $\sigma(t)$ is of concern, however; it is readily found from Eq. (20) by noting that the maximum value of the quantity in braces is 2. Hence, $\sigma_{MAX} = \pi\, c\tau/[s^2(1/a + 1/H)]$.

To study the leading edge versus sea state, we use parameters typical of a Skylab satellite altimeter: $H = 435$ km, $\psi_B = 1.5°$, and $\tau < 15$ nsec. In addition, we use Eqs. (18) to relate the statistics of the wind-excited surface to wind speed. The result is the family of normalized curves shown in Fig. (4), showing the leading edge of the return. The mean surface, of course, is located at $t = 0$, which appears at precisely one-half the maximum value. The effect of sea state is as expected; higher wind speeds and hence greater rms roughness heights tend to stretch (i.e., disperse) the leading edge, giving a greater rise time.

3. Beam-Limited Altimeter ($\psi_B \ll \sqrt{c\tau/H'}$)

In less frequent altimeter applications, the configuration may be beam-limited, as shown in Fig. 3(b). In this case, the interaction at the surface directly beneath the altimeter appears planar, i.e., the effects of the spherical earth and spherical pulse front are negligible. This could occur for a low-flying, narrow-beam aircraft altimeter, but would not exist for a satellite altimeter. When this extreme is achieved, the return can best be analyzed by expanding the second term in Eq. (20) in a Taylor series, expanded about argument $ct/(\sqrt{8}\ \sigma_h)$. This gives

$$\sigma(t) \simeq \frac{c\tau H^2 \psi_B^2}{2\sqrt{2\pi}\, s^2 \sigma_h} \left[e^{-\left(\frac{ct}{\sqrt{8}\ \sigma_h}\right)^2} + \cdots \right] , \qquad (21)$$

where the higher-order terms omitted here are of the order of $H'\psi_B^2/\sqrt{8}\ \sigma_h$, which is assumed to be small since we have taken $c\tau/2 < 2\sigma_h$.

The maximum and the Gaussian nature of this return are easily seen from the above equation. The width of the pulse is directly related to the rms surface height, and the mean position of the surface occurs precisely at the pulse peak.

DEDUCTION OF MEAN SURFACE POSITION AND SEA STATE FROM ALTIMETER RETURN

If we can employ a beam-limited short-pulse altimeter, we will have no trouble deducing either the mean surface position or the rms surface height of the ocean. The former is found from the pulse peak position and the latter from its width, as readily observed from Eq. (21). Unfortunately, the parameter requirements for this limiting configuration are such as to preclude its implementation on a satellite.

Restricted, then, to pulse-limited altimeter operation from a satellite, the question remains as to how to find the mean surface position in the leading edge of the extended echo. From Eq. (20) and the curves plotted in Fig. 4, the answer is obvious--in the absence of noise. Merely find the half-power point on the rising edge; this time corresponds to the distance to the mean surface. However, in the presence of additive, independent noise, and with the often-jagged appearance of the echo near its maximum (see measured returns in Fig. 6), finding this half-way point becomes more difficult.

A signal processing technique to be suggested here makes use of the fact that this half-power point defining the mean surface position is also the point of maximum slope. Hence, we suggest that the processor form the time derivative of the altimeter output power--after incoherent averaging (or summing) and band-pass filtering of several pulse returns. Thus, the incoherent averaging and filtering will remove much of the jagged noise, while providing a smooth, clearly recognizable leading edge. The derivative of this signal is easy to form from Eq. (20). It is

$$\sigma'(t) = \sqrt{\frac{\pi}{2}}\,\frac{c\tau}{2s^2}\cdot\frac{c}{\sigma_h\left(\frac{1}{a}+\frac{1}{H}\right)}\,e^{-\left(\frac{ct}{\sqrt{8}\,\sigma_h}\right)^2} \qquad (22)$$

Figure 5 shows a family of normalized curves of this average altimeter leading-edge output differentiated versus time. The pulse center is the mean surface position, and its width is clearly proportional to rms surface height (or the square

C4

of wind velocity, for wind-driven waves). There is no need for absolute measures of signal level, either for mean surface position or for sea state determination; hence, atmospheric attenuation and system power drifts are not critical.

A large amount of noise can, of course, degrade the pulse positioning accuracy of this system, as in any system. However, so long as σ_{MAX} is several decibels above the noise level, the position of the pulse center in the signal derivative should be relatively insensitive to noise. The degradation of altimeter accuracy with sea state and noise level has the desirable attributes of pulse-position modulation (PPM) systems of digital communication theory, but should be the subject of further study.

COMPARISON OF THEORETICAL MODEL WITH GROUND-TRUTH DATA

For verification of the theory and the various assumptions that have gone into it, we choose measured data from two separate altimeter experiments: one pulse-limited and the other beam-limited. The pulse-limited data chosen was measured and reported by Raytheon[6] for aircraft flights at 10,000 ft with a pulse width of 20 ns. The half-beamwidth, ψ_B, is 2.5°, and the surface winds reported during Flights 14 and 16 were 12 and 22 knots, respectively. Their averaged altimeter outputs are shown in Fig. 6. Since there is no precise way of comparing measured surface position with that calculated, we intend to compare the actual sea state effects, as contained in the leading-edge rise time, t_r, with those calculated. We roughly measure rise times of 21 and 30 ns for the two records displayed, and use Eqs. (18) and (20) to calculate the wind speeds required to cause seas producing this rise time. The calculated winds are 14.1 and 21.2 knots, comparing reasonably well with the measured winds. Good comparison on Flight 14 was not expected, because the condition $c\tau/2 > 2\sigma_h$ is barely satisfied for this mild sea condition. When this inequality is not satisfied, Eq. (20) is not applicable, and one must instead go back to Eq. (19). Practically, this means that with a 20 ns pulse, one cannot hope to meaningfully measure sea states which will produce a rise-time stretching of less than 20 ns.

As an example of the comparison of Eq. (21) for beam-limited operation with measurements, we selected data recently reported by Yaplee et al[7]. His measurements were taken from a tower at H = 70 ft above the water and $\psi_B \simeq 1°$. His pulse width $\tau = 1$ ns was long enough to assure beam-limited operation, but short enough to allow

the condition $c\tau/2 < 2\sigma_h$ to be satisfied for the two sets of data reported. We compare the shapes of the curve given by our Eq. (21) with what he has called the impulse response* shown in his Figs. 11 and 12. He plots the responses measured both by radar and by a wavestaff, for two different days on which the significant waveheights (measured by the wavestaff) were 3.1 and 5.2 ft. Since his response heights were relative, we compare the shape of his curves in Fig. 7 with that of our Eq. 21, using rms waveheight, σ_h, corresponding to 3.1 and 5.2 ft. The agreement in width is quite good. The comparison also points out where the Gaussian assumption for the sea height is weak: in the echo tails and in the symmetry about the center. The Gaussian surface has some (small) probability of very large heights, and is always symmetric, whereas the height of real ocean waves can never be infinite, and the surface is not exactly symmetric for positive and negative heights. These differences, while interesting, should not detract from the fact that the simple Gaussian model can be applied adequately well to predict mean surface position and rms waveheight.

CONCLUSIONS

The principal conclusions to be made from this analysis are that a short pulse altimeter can be used--even in the presence of high seas--to measure accurately the mean surface level and also to deduce the sea state. The simple interaction of the microwave altimeter pulse with the sea at near-vertical incidence is separable from the more complex interaction mechanism at larger incidence angles; It follows the straightforward specular point theory derivable from either geometrical or physical optics.

In satellite applications, the altimeter return will be pulse-limited in its nature. For reasonably meaningful measurements of the geoid, the pulse width must be kept small, i.e., less than 20 ns. It is precisely for these short pulses that ocean waveheights can temporally disperse the signal leading edge. We have shown by the specular point theory, however, that this interaction is known and its results are predictable. We have suggested and discussed a signal processing scheme employing the signal derivative, which can locate the mean surface position from the pulse position and the rms surface height from the pulse width.

*The impulse response essentially has the effect "deconvolving" the pulse shape and size from the return to give a result with the same meaning as our Eq. (21).

Comparison of the theory with measurements and ground-truth data for two different altimeter modes (pulse- and beam-limited operation) lend credence to the theory. System noise can and will limit altimeter accuracy, but this can be reckoned with in a systematic manner using principles of PPM communication theory. Other practical effects such as nonrectangular pulse shapes can be accounted for in any further system analysis by including an additional pulse-shape factor in the integrand of Eq. (19).

In short, the pulse-sea interaction is at present sufficiently well understood and verified that a short-pulse altimeter could be built which will provide: (1) accurate determination of mean sea level to a precision much greater than ocean waveheights, and (2) as a by-product, can provide rms ocean wave height (or wind speed) as well.

ACKNOWLEDGMENT

The analytical assistance and constructive comments of T. Kaliszewski are gratefully acknowledged.

REFERENCES

1. J. A. Greenwood, A. Nathan, G. Neumann, W. J. Pierson, F. C. Jackson, and T. E. Pease, "Radar altimetry from a spacecraft and its potential applications to geodesy", Remote Sensing of the Environment, vol. 1. New York: American Elsevier Publishing Co., Inc., 1969, pp. 59-80.

2. T. W. Godbey, "Oceanographic satellite radar altimeter and wind sea sensor", from Oceanography in Space, Proc. of Conference, Woods Hole Oceanographic Institution, Ref. No. 65-10, G. C. Ewing, Ed., Aug. 24, 1964, pp. 21-26.

3. D. E. Barrick, "Rough surface scattering based on the specular point theory", IEEE Trans. Antennas Propagat., vol. AP-16, 1968, pp. 449-454.

4. R. D. Kodis, "A note on the theory of scattering from an irregular surface", IEEE Trans. Antennas Propagat., vol. AP-14, 1966, pp 77-82.

5. O. M. Phillips, Dynamics of the Upper Ocean. London: Cambridge at the Universit Press, 1966, pp. 109-139.

6. ———, "Space geodesy aircraft experiment", Raytheon Co., Wayland Laboratories, Sudbury, Massachusetts, Final Rept., Contract No. NASW 1932, May 1970.

7. B. S. Yaplee, A. Shapiro, D. L. Hammond, B. D. Au, and E. A. Uliana, "Nanosecond radar observations of the ocean surface from a stable platform", IEEE Trans. Geoscience Electronics, vol. GE-9, 1971, pp. 170-174.

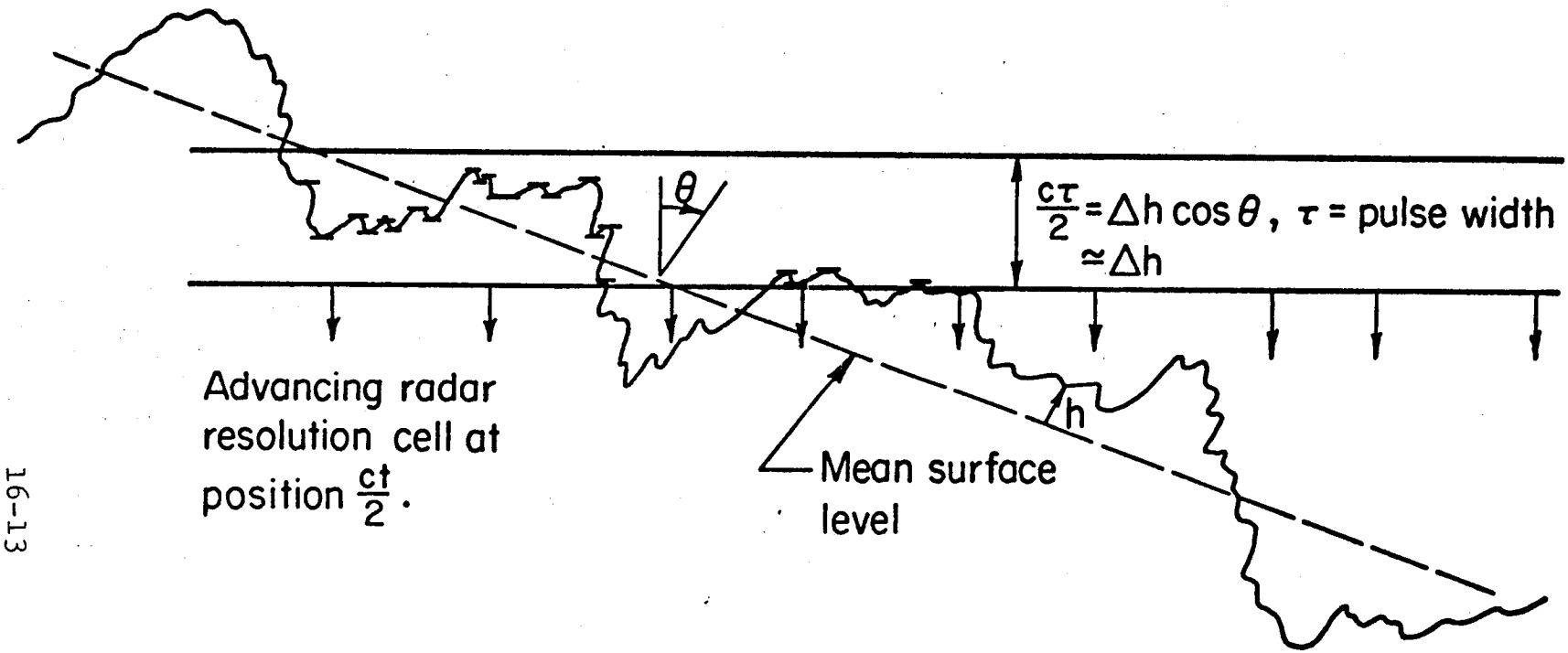

Figure 1. Physical Picture of Specular Point Scatter. Specular Points Within Radar Resolution Cell Are Shown Highlighted.

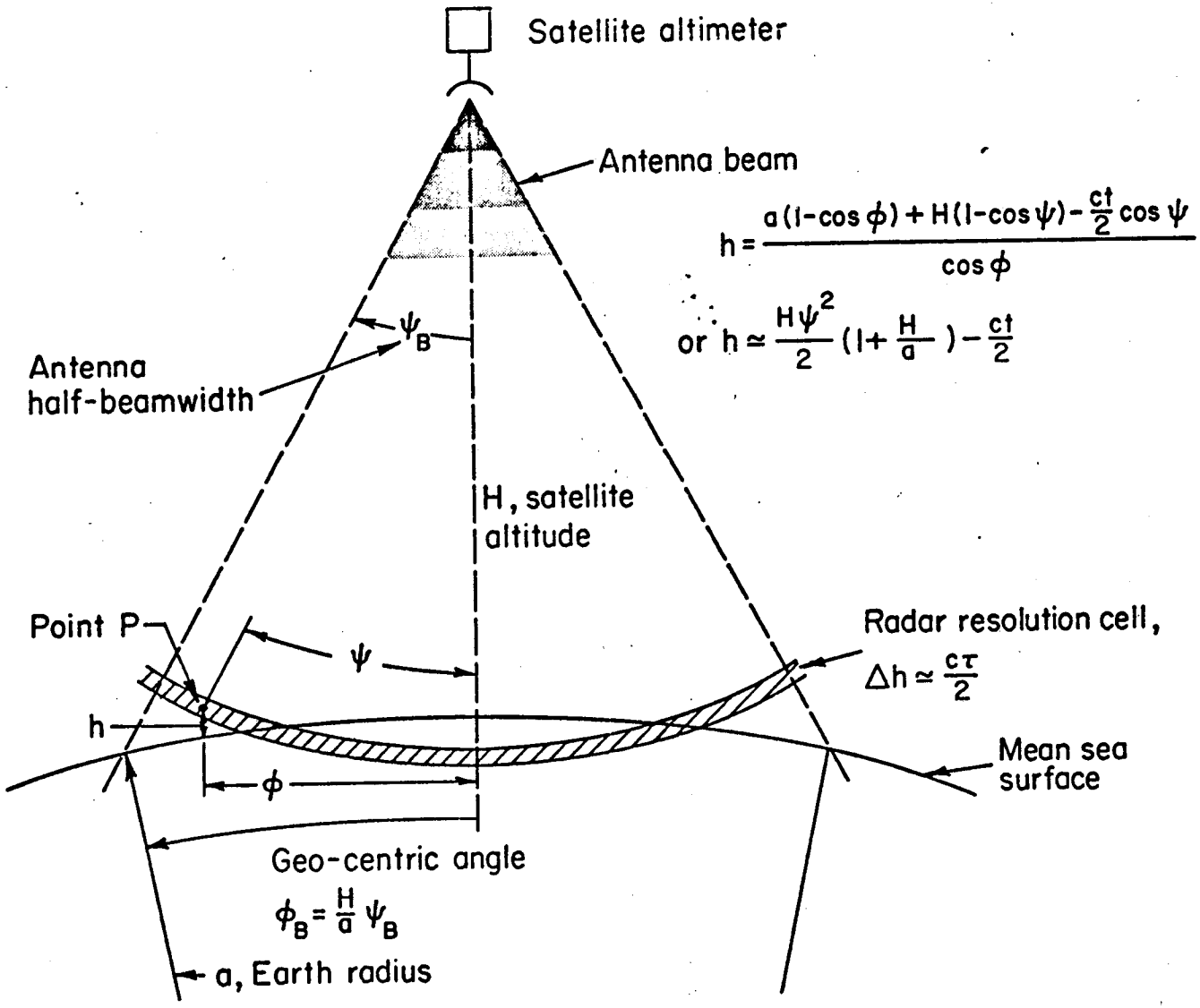

Figure 2. Geometry of Satellite Altimeter

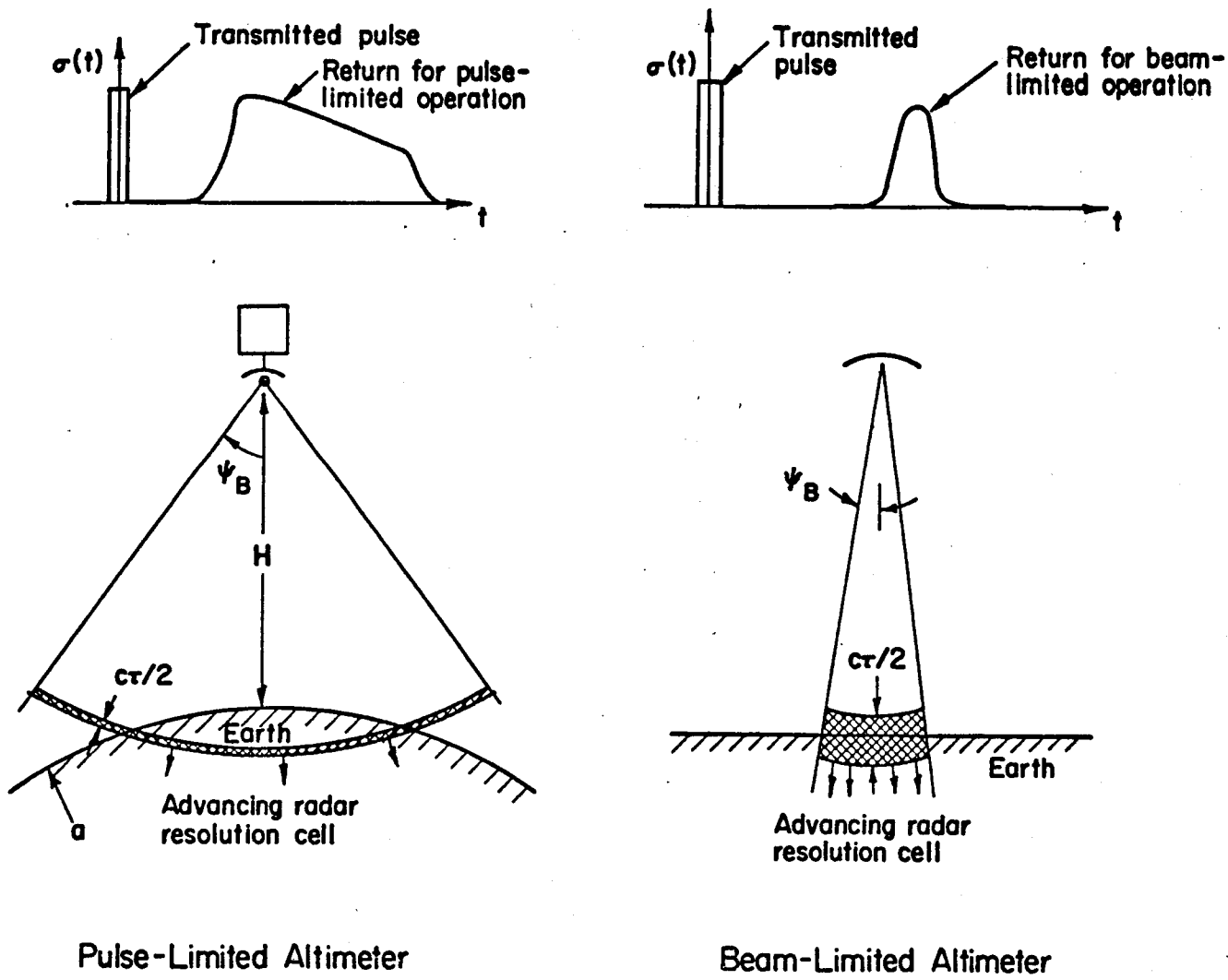

Figure 3. Two Modes of Altimeter Operation and the Resulting Signals

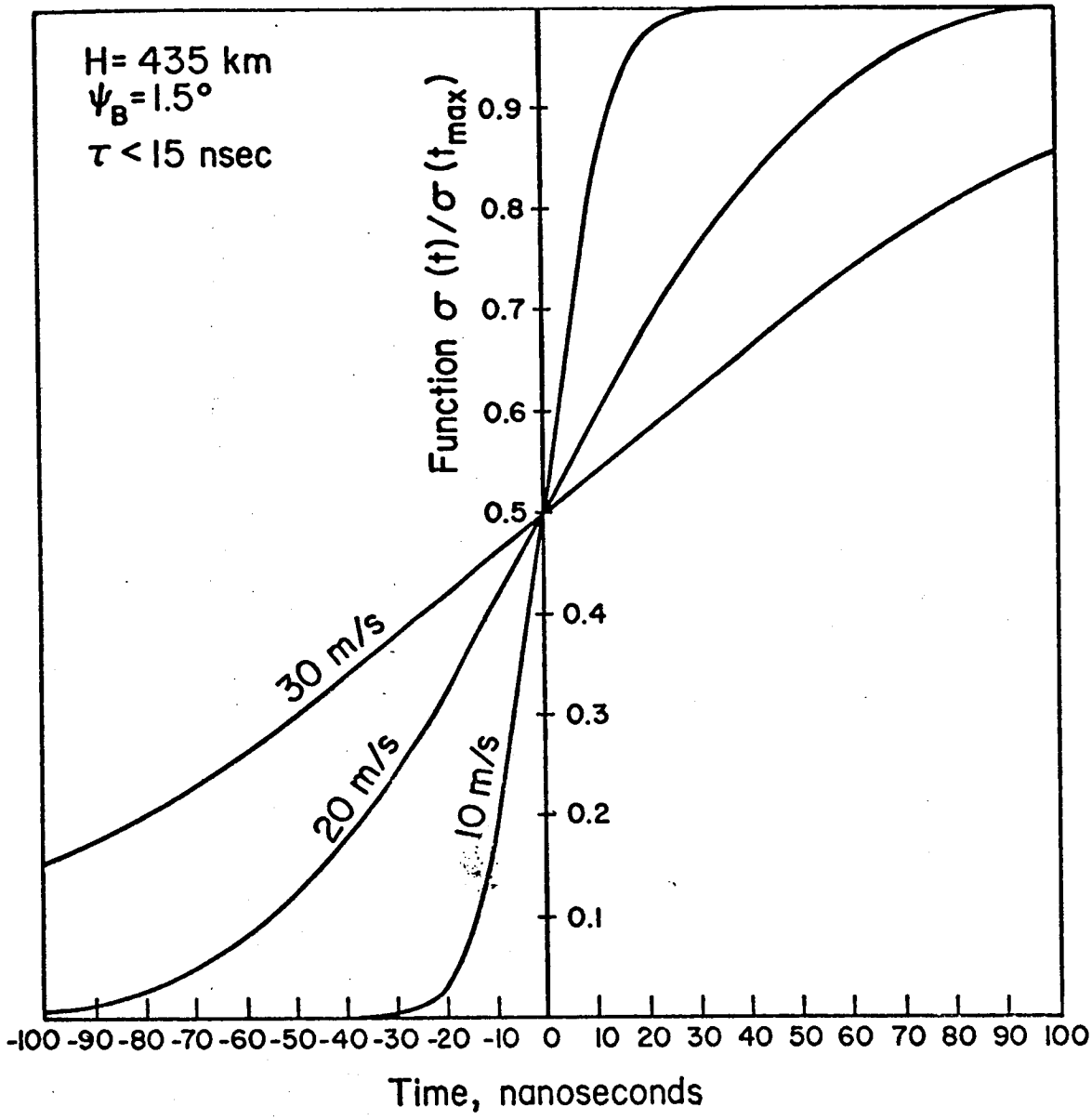

Figure 4. Leading Edge of Averaged Altimeter Output Versus Time for Pulse-Limited Operation

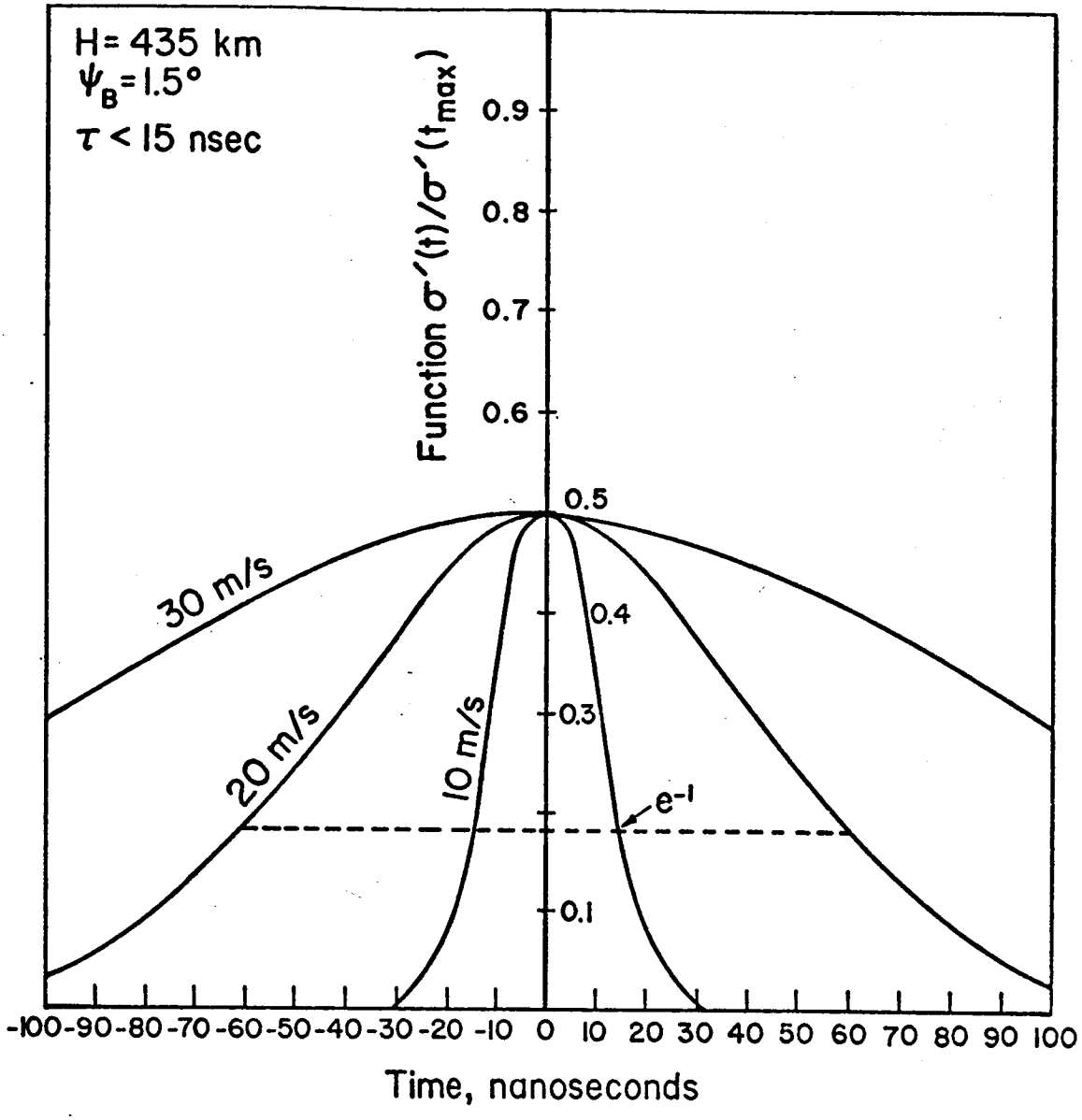

Figure 5. Derivative of Leading Edge of Averaged Altimeter Output Versus Time for Pulse-Limited Operation.

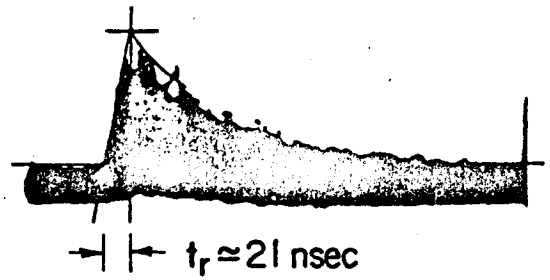

Flight #14
Run #12
H = 10 kft
τ = 20 nsec
$t_r \simeq 21$ nsec
Measured wind = 12 knots
Calculated wind = 14.1 knots

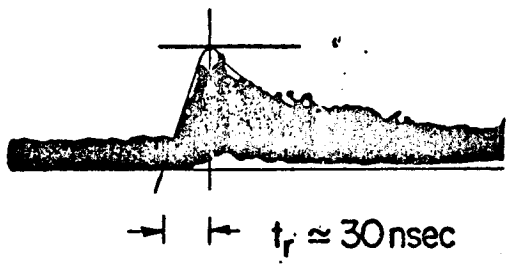

Flight #16
Run #9
H = 10 kft
τ = 20 nsec
$t_r \simeq 30$ nsec
Measured wind = 22 knots
Calculated wind = 21.2 knots

Figure 6. Measured [Raytheon Co., Wayland Laboratories, 1970] Aircraft Altimeter Responses. Wind Speeds Inferred from Rise Time and Pulse-Limited Model Are Compared to Observed Wind Speeds.

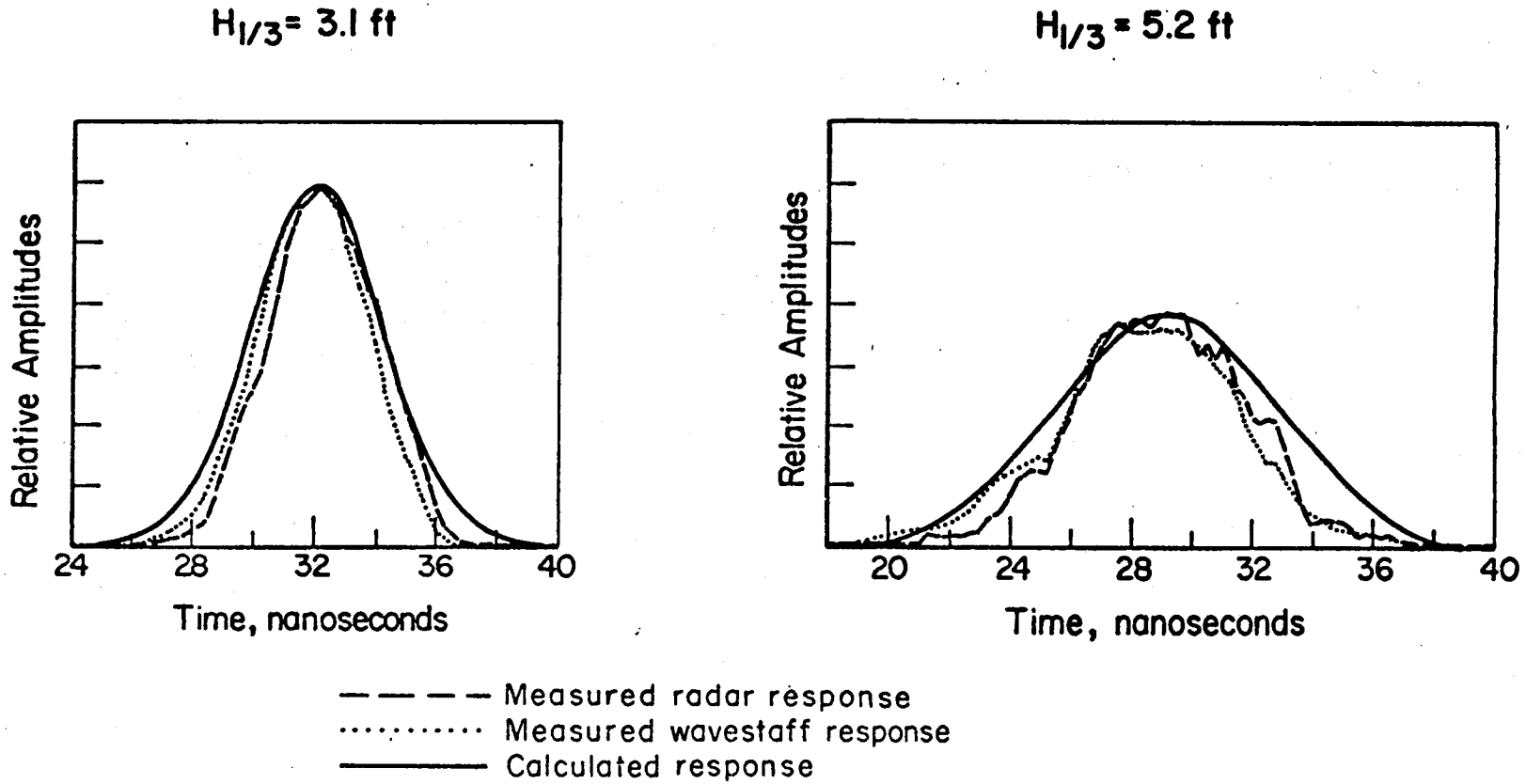

Figure 7. Measured [after Yaplee et al, 1971] Altimeter (Impulse) Responses Versus Calculated Using Beam-Limited Model